Self-Assembly of Platinum Nanoparticles of Various Size and Shape†

Janet M. Petroski, Travis C. Green, and Mostafa A. El-Sayed*

Laser Dynamics Laboratory, School of Chemistry and Biochemistry, Georgia Institute of Technology, Atlanta, Georgia 30332-0400

Received: May 24, 2000; In Final Form: February 6, 2001

The addition of dodecanethiol to a polydisperse platinum colloidal aqueous solution capped with acrylic acid leads to self-assembled monolayers which not only contain various sizes, but also various shapes of nanoparticles. Assembled monolayers arranged in hcp arrays are achieved for mixed shape samples. In the case of the assembly of cubic nanoparticles, cubic closest packing is achieved when the size difference between the nanoparticles is less than 25% (or between 6 and 8 nm). The ccp array is disrupted when the size difference is between 25 and 60% or there is a mixture of shapes. Finally, size segregation is seen in regions where the size difference is more than 60% with the resultant assembly being hcp no matter what the shape.

Introduction

The ability of colloidal solutions of metal and semiconductor nanoparticles to spontaneously form ordered arrays has been a research area of concentrated study. Not only have various types of nanoparticles been assembled from metals to semiconductors but also the assembly has been achieved using a variety of organic and biological materials.[1−7] The nanoparticles reported in the literature which form self-assembled monolayers (SAMs) all contain common particle characteristics: small average diameters, narrow size distributions, similar shapes, alkyl stabilizing agents, as well as organic solvents. In each case, the capping agent played a key role in influencing the ordered packing.

Our group has been able to synthesize aqueous colloidal solutions of platinum nanoparticles with various shapes by using hydrogen gas as the reducing agent and water as the solvent.[8,9] The dominant shapes which have been synthesized are cubes which have 6 {100} faces, tetrahedra comprised of 4 {111} faces and truncated octahedra consisting of 6 {100} and 8 {111} faces. To use these nanoparticles in any new material application, their self-assembly becomes important. None of the above desired characteristics for self-assembly are present in these shape selective Pt nanoparticles. Although the dominant shape of the resultant nanoparticles can be controlled, the size distribution and the mixture of shapes inherently present in this synthetic method have made the long range assembly of these nanoparticles a difficult process. The polyacrylate polymer used as the capping material inhibits closest packing from occurring. Also complicating matters is the use of water as the solvent. The spontaneous assembly evident with organic solvents cannot be achieved here since the evaporating time increases from approximately 10−20 min to 1−2 h. Furthermore, the water solvent does not lend itself to the size selective precipitation methods used to narrow the size distributions of the nanoparticles synthesized in hydrophobic solvents. It is not known how the properties of hetero-assembled nanoparticles will affect the ordering of the monolayers. It is thus important to study the requirements needed for assembling polydisperse solutions such as those produced by this synthesis. The extent of organized structures obtained and the difference in packing arrays between heterogeneous and shape selected samples are explored.

Because of the large size of the polyacrylate capping material used (MW ∼2100), a closest packing array of these nanoparticles could not be achieved. Therefore, the first step in attempting to assemble these nanoparticles was to synthesize them using a capping material of smaller size that would still produce the shapes required. As had been previously reported,[10] the polyacrylate plays a key role in controlling the shape of these nanoparticles by acting as a buffering agent during the growth period. Acrylic acid was chosen since it is essentially the monomer unit of the polyacrylate and does possess the same buffering characteristics required for a capping material in this synthetic method if added in large amounts. As with the polyacrylate, the ratio of the acrylic acid to that of the platinum salt determined the final shape distribution of the nanoparticles. These samples afforded us a unique opportunity to study not only the effect shape had on the ability of these nanoparticles to assemble, but we could also investigate the effect of size on the ordering of these nanoparticles while keeping the shape relatively constant. There have been accounts in the literature[11,12] of gold spherical nanoparticles assembled with various sizes. The cubic nanoparticle assemblies are compared to these references to further explore the influence of size on the packing of nanoparticles.

The kinetics of aggregation for colloidal solutions of metal nanoparticles has been well documented in the literature.[13−16] Generally, these solutions will undergo diffusion-limited aggregation which is characterized by the tenuous chainlike structures or fractals. These types of structures generally do not form ordered arrays. Therefore, two modifications were employed to aid in the assembly of these nanoparticles. The first change was to extend the drying time allotted to the solution samples applied to the TEM grid since the evaporation rate of the solvent was found to drastically influence the extent of particle aggregation. In the second adjustment, the colloidal solution was modified by the addition of dodecanethiol (thiol). The addition of the thiol into the solution allowed the aggregation process to become ordered into closest-packed arrays. The size and shape of the nanoparticles determined the type of

† Part of the special issue "Edward M. Schlag Festschrift".

* Corresponding author.

10.1021/jp0019207 CCC: $20.00
Published on Web 03/22/2001

packing that resulted. For the mixed sample, the ordering resulted in hexagonally closest packed (hcp) arrays. For the cubic sample, the areas where the particle size distribution was narrow (difference of ~25%) resulted in SAMs of cubic closest packing (ccp) arrays. In the areas where there was a large size distribution, and/or other shapes present, the resultant ccp SAMs were disrupted and sometimes randomness prevailed. Hexagonally closest packing was seen in regions containing a large shape distribution, similar to the mixed sample. This hcp is further observed in areas where the smallest nanoparticles (the size of the nanoparticles was on the order of the size of the dodecanethiol) were segregated by their size into their own arrays. In these regions the packing was independent of shape.

Experimental Section

Pt nanoparticles were prepared by using the technique of Rampino and Nord[17] and Henglein et al.[18] This synthesis uses acrylic acid as the capping material and was closely based on the previously described preparation using polyacrylate as the capping material.[7] For the synthesis of cubic nanoparticles, 0.8 mL of a prepared 1.0 M acrylic acid solution (acrylic acid, sodium salt, Aldrich, 97%) was added to an aged solution of 8×10^{-5} M K_2PtCl_4 (Aldrich, 99.99%) prepared in 250 mL of water, giving a 1:40 ratio of Pt:acrylic acid. Ar gas was then bubbled through the solution which was adjusted to an initial pH of ~7 and reduced by flowing H_2 gas through the solution. The kinetically controlled growth of the nanoparticles took approximately 12 h. The synthesis of the mixed shape solution was prepared the same way except only 0.4 mL of 1.0 M acrylic acid was used, yielding a 1:20 ratio of Pt:acrylic acid.

TEM samples from Pt solutions were prepared by adding a drop of the Pt solution to a TEM grid. Under ambient conditions, the drop would dry in less than 2 h and lead to agglomerations of nanoparticles. However, to reduce the evaporation rate of this sample drop one of two techniques was used (both provided similar results). In the first, a drop of the Pt nanoparticle sample was added to a TEM grid in a sealed environment with a saturated salt solution. In this humidity (98%) chamber, the visible drying time was increased to over 6 h. The second method involved adding successive drops of the H_2O solvent to a sample TEM grid, under ambient conditions, after approximately half of the original sample drop had evaporated. This was then repeated several times until the total drying time was over 4 h.

Dodecanethiol additions were made by injecting 10 μL of thiol into 5 mL of the final Pt nanoparticle product in solution followed by vigorous stirring for 10 min. Although the thiol is immiscible in the H_2O Pt solution, the mixing did allow for adsorption of the thiol on the surface of the particles allowing for SAMs to form. All samples containing thiol were imaged after slow solvent evaporation techniques.

TEM was performed at 200 kV from a high field emission source Hitachi HF 2000 TEM. The TEM grids used in these experiments were copper 200 mesh Formvar carbon from Ted Pella, Inc.

Results and Discussion

Figure 1 shows a TEM image of a mixed shape sample before the addition of thiol. The average size for the particles is ~6 nm with diameters ranging from approximately 2 to 11 nm. The shape distribution was found to be approximately 36% tetrahedra, 30% cubes, and 34% truncated octahedra (over 400 nanoparticles were counted for the distribution). The image contains regions of monolayers of particles which is an example

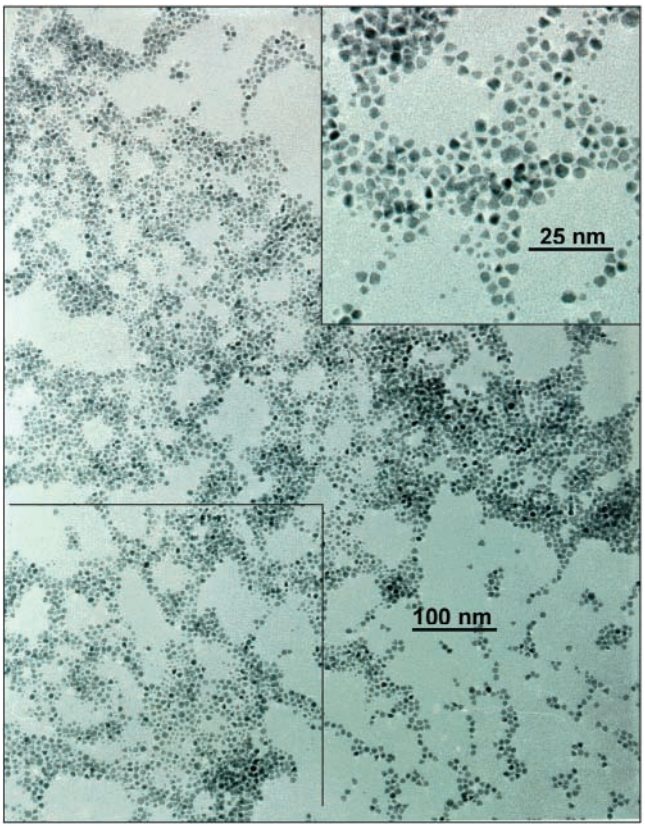

Figure 1. TEM image of a 1:20 ratio Pt:acrylic acid mixed shape sample depicting fractal-like growth before the addition of dodecanethiol. The inset is an enlarged region of the figure depicting the short-range order of the nanoparticles.

of the slow-solvent evaporation method described previously. However, the overall assembly is characterized by the complex structures which do not form extended ordered arrays. It should be noted that in this figure, as in most of the subsequent images, some particle aggregation and, in some cases, three-dimensional structures are evident. This is common in most assembly techniques over a long range such as these figures show and will not be further examined here. The inset shows an enlarged portion of the figure to depict the short order range of the individual nanoparticles. Interactions between {111} faces, {100} faces, and {111}-{100} faces between the TO and tetrahedral nanoparticles were observed for these densely packed samples. The interactions are generally taking place between nanoparticles of like faces. For example, a cube with a {100} face generally will align next to another cube or the {100} face of a truncated octahedron. One of the {111} faces of the truncated octahedron may align with a tetrahedron {111} or another truncated octahedron. It is rare that a {111} and a {100} face align. When this happens, the spacing between the nanoparticles is usually greater than the average.

Figure 2 depicts a TEM image for the same mixed shape sample shown in Figure 1 after the addition of thiol. It is clearly evident that the fractal formation no longer occurs and is replaced by the formation of SAMs. These monolayers are arranged in hcp arrays. Another notable difference from dodecanethiol addition was an increase in the distances between adjacent particles. This increase in the interparticle distance is evident in the inset, which is an enlarged region of the figure. Here the face-to-face alignment of the nanoparticles is not as prevalent as Figure 1.

Figure 3 shows a typical TEM image of a platinum colloidal solution, comprised of over 70% cubes, which is characterized

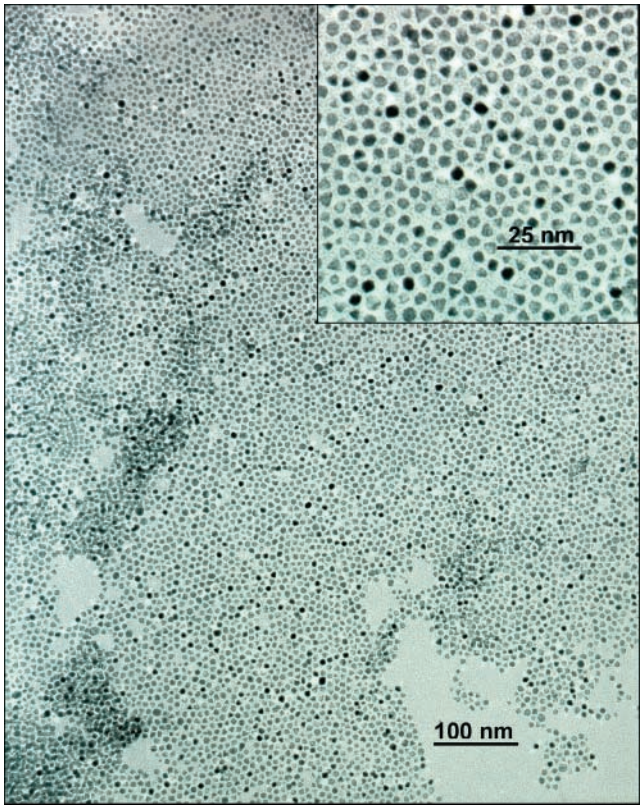

Figure 2. TEM image of 1:20 ratio Pt:acrylic acid mixed shape samples with thiol added to the same solution from Figure 1. The formation of assembled monolayers displaying hexagonally closest packing arrays is evident. The inset is an enlarged region of the figure depicting the short-range order of the nanoparticles.

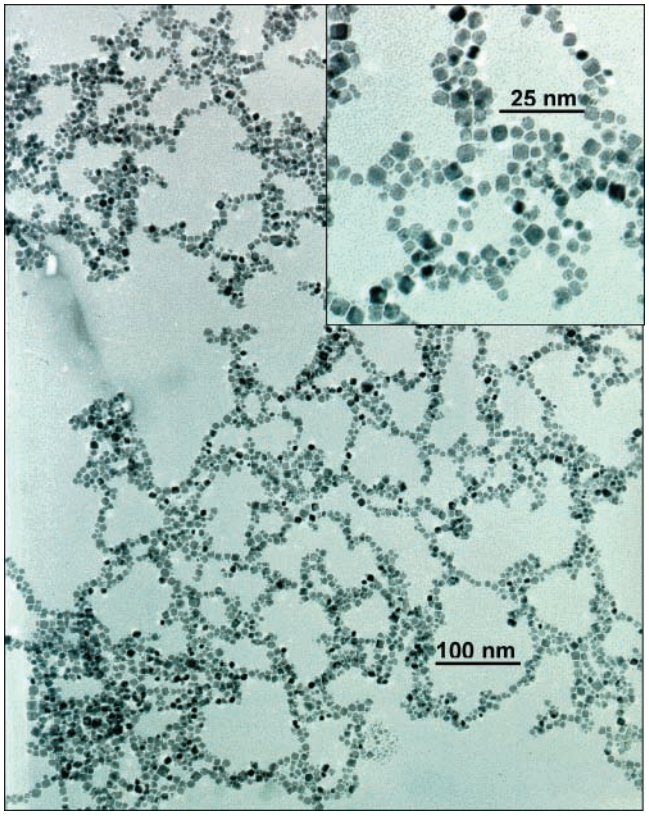

Figure 3. TEM image of 1:40 ratio sample depicting fractal-like growth before the addition of dodecanethiol. The inset is an enlarged region of the figure depicting the short-range order of the nanoparticles.

by the chainlike fractal formation. As with the mixed sample of Figure 1, these solutions do not form ordered arrays. The average size of the particles is ~7 nm with diameters ranging between 2 and 12 nm. As with Figure 1, face-to-face interactions are observed in the inset of an enlarged region of the figure.

Figure 4 shows TEM images of the same solution seen in Figure 3 after the addition of dodecanethiol. These images were taken from neighboring regions of the same TEM grid. Although the addition of thiol allowed the nanoparticles to order into closest-packed arrays, the size of the nanoparticles determined the type of packing that resulted. In regions where the particle size distribution was narrow (Figure 4a), the SAMs which resulted were of cubic closest packing clusters. There are large areas between the clusters where no particles are present. In the regions where there was a large size distribution and/or mixed nanoparticle shapes (Figure 4b), the resultant ccp SAMs were disrupted and in some instances seem to form hexagonal closest packing arrays which covered a large area of the TEM grid. The hcp is more evident for regions of very small nanoparticles. As was observed in the mixed sample, there is an increase in the interparticle distance from Figure 3. The addition of thiol seems to assist greatly in the formation of SAMs of nanoparticles of different shapes and sizes. This might be possible due to the fact it introduces more stabilizing dispersion forces between the capping molecules. It is also possible that the addition of thiol reduces the rate of water evaporation to allow for better formation of low energy SAMs.

To determine the effects of interparticle distances due to acrylic acid and thiol capping adsorbed to the particle surface, the distances between particles were measured for a mixed sample and shown in Figure 5. For samples without thiol, distances between particles were due to acrylic acid capping. Measurements were obtained from nanoparticle−nanoparticle interactions oriented along their {100} or {111} faces. For comparison with the sample in the presence of thiol, only the distances between particles that were self-assembled in organized arrays were measured. Determining the distances between oriented and ordered particles ensures that the separation was due to adsorbed acrylic acid or dodecanethiol molecules. The results shown in Figure 5 indicate that the average interparticle distance increased from 1.19 ± 0.2 nm to 2.25 ± 0.2 nm upon the addition of dodecanethiol to Pt nanoparticle solutions. It should be emphasized that the interparticle distance is independent of the shapes or sizes of the particles measured. Furthermore, the same distances were found for both the mixed and cubic nanoparticle samples and is therefore also independent of the concentration of the acrylic acid in the sample.

The calculated length of the acrylic acid molecule is ~0.6 nm. The average interparticle distance of 1.19 nm measured between adjacent acrylic acid capped particles suggests that two layers of capping material (one for each particle) separates the adjacent particles. Upon the addition of thiol, the average distance measured between adjacent particles increases to 2.25 nm. This interparticle distance is slightly longer than the 17 Å that had been reported previously for gold.[19] Since the acrylic acid capping material is still present in these solutions, it is proposed that the thiol group is passivating the surface along with the acrylic acid capping material. These two combined molecules account for the additional space between the nanoparticles.

Polydisperse solutions of gold nanoparticles of a single spherical shape have been studied previously along with the role of the dodecanethiol in the assembly process. The concept of the nanoparticles as "soft spheres" which order with an effective hard sphere diameter was introduced to explain the

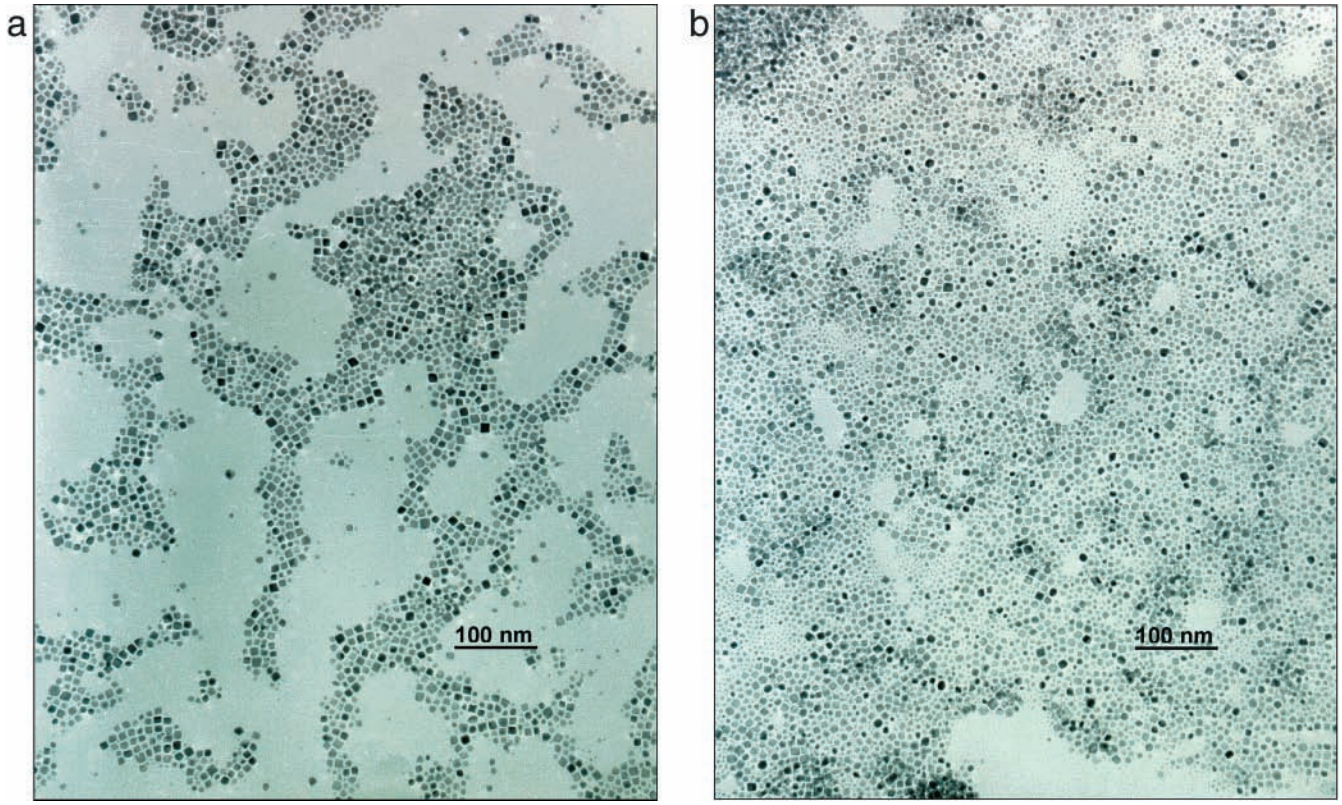

Figure 4. a) TEM image of 1:40 ratio samples with thiol of narrow size distribution depicting crystals of cubic closest packed (ccp) arrays; and (b) TEM image of 1:40 ratio samples with thiol of large size distribution depicting crystals of disrupted ccp regions (seen by the curving of the relatively straight ccp).

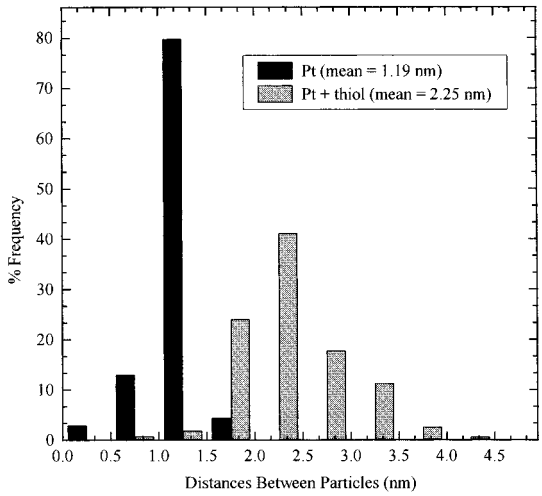

Figure 5. Histogram showing the interparticle distances between face-to-face oriented particles without thiol addition and ordered particles after the addition of thiol. The distance between nanoparticles with only acrylic acid capped to the surface is 1.19 ± 0.2 nm. The distance increases to 2.25 ± 0.2 nm for ordered particles with both acrylic acid and thiol present.

assembly achieved by thiols.[20,21] These soft spheres differ from hard spheres because the rigid metallic cores are surrounded by soft capping ligands. In the case of these platinum nanoparticles, the addition of the thiol into the colloidal solution passivates the particle's surface much more extensively than the acrylic acid alone thus creating "soft shapes". But the shape of the nanoparticle still allows the core structure of the different faces to affect the ordering.

Heath et al.[11] used a solution consisting of dodecanethiol-passivated gold nanoparticles with a large size distribution. They found that the largest nanoparticles tended to seed the growth of the rest of the cluster with the smaller nanoparticles

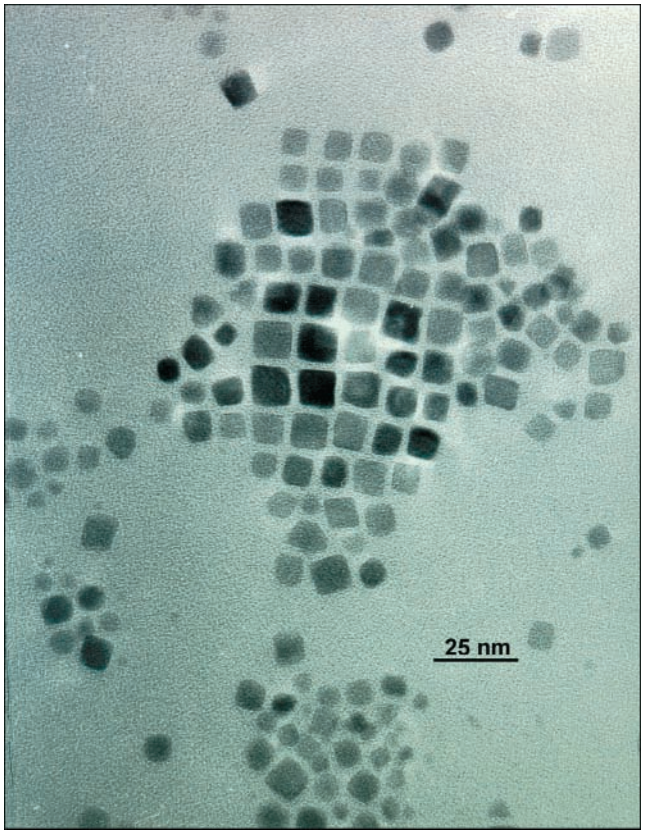

Figure 6. TEM image of a single cluster of approximately 100 cubic platinum nanoparticles organized into a ccp assembly.

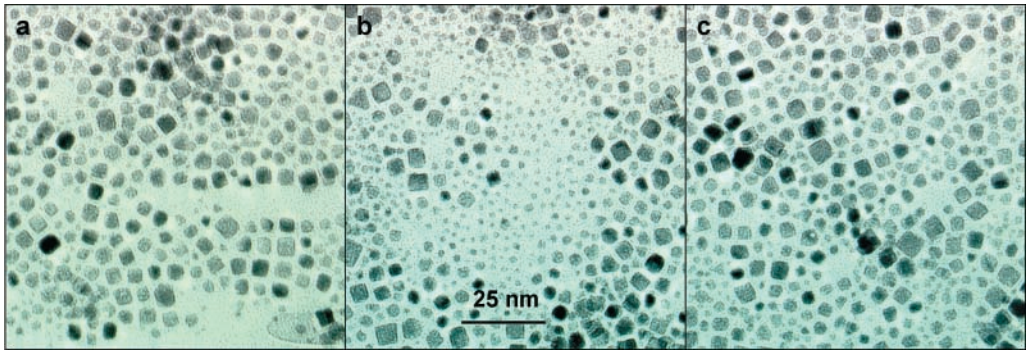

Figure 7. Enlarged regions of the TEM image of 1:40 ratio sample with thiol of large size distribution (Figure 4b). (a) depicts the ccp assembly of nanoparticles of similar size, (b) shows the size segregation due to the large difference in the ratios of the nanoparticles resulting in hcp for the smallest nanoparticles, and (c) shows the disruption of the ccp assembly due to nanoparticles of various shapes and sizes.

assembling around the larger ones instead of forming their own separate assembly. This type of cluster growth was attributed to the size-dependent dispersion forces of the nanoparticles which formed well-ordered hcp clusters. Therefore, it was concluded that it is the size dependence of the energetics which leads to the radial size segregation. Figure 6 depicts this phenomenon with the cubic platinum nanoparticles. This cluster consists of approximately 100 nanoparticles. It is evident that the cubic nanoparticles of like size organize into ccp regions until the smaller cubes or other shaped nanoparticles try to assemble around this cluster. This disrupts the cubic packing, and if the cluster continues to grow with the smaller nanoparticles surrounding the larger cubic nanoparticles, the resultant packing becomes almost hcp, depending on the size of the nanoparticles.

Kiely et al.[12] have demonstrated the size effects on the assembly of gold spherical nanoparticles with a decanethiol passivated surface. In this work, nanoparticles of two different known sizes were mixed together. It was found that the size ratio of the two nanoparticles determined the type of assembly formed. If $R_A/R_B \geq 0.8$, where R_A and R_B are the radii of the smaller and larger nanoparticles, respectively, then the nanoparticles assembled into hcp organizations. For $0.6 \geq R_A/R_B \leq 0.8$, the nanoparticles would still assemble as hcp, but the smaller nanoparticles would now fit in the interstitial sites forming separate hcp arrays of the two sizes. For $R_A/R_B \leq 0.4$, the two sizes formed phase segregated clusters with no mixing occurring.

Similar results are shown for the cubic platinum nanoparticles in Figure 7 which consists of enlarged areas of Figure 4b. Unfortunately, this experiment was not as controlled as the above gold experiments. There is a range of sizes present (not just two different sizes) in these TEM images due to the nature of the synthesis and the polydispersity of the resulting solutions. But, all of the above observations can be seen in a single TEM image like Figure 4b. In Figure 7a, the nanoparticles are of similar size (between ~6 and 8 nm) and organize into a ccp array, which is also seen in Figures 4a and 6. The maximum size difference in these nanoparticles is ~25%. It can be noted that the size of the cubic nanoparticles which participate in this type of assembly make up almost half of the total nanoparticles present in the colloidal solution. This organization continues until nanoparticles of smaller size or different shape assemble around this cluster and disrupt the packing, as described above.

In Figure 7b, the assembly of the smallest nanoparticles (~2 nm) is separated from the other nearby nanoparticles (average of ~6 nm). Therefore, the phase segregation evidenced in gold is also evidenced here. Also of note is the fact that these small nanoparticles assemble by hcp even when there is a mixture of tetrahedral and truncated octahedral shapes along with the cubic ones. The size of these nanoparticles are on the same order as the interparticle distance, or the length of the thiol molecule. This may affect how the shape of the nanoparticle is perceived by its neighbors (the nanoparticle may be more like a soft sphere than a soft cube). The assembly seems to be driven more by the energetics of the packing type itself and it is proposed that the nanoparticle shape has less to do with the assembly in this size range. This spherical-like behavior leads to the hcp arrays for these small nanoparticles.

The interstitial site packing is not evidenced to the same extent in this image, probably because of the extensive ccp assembly which does not have interstitial sites like those of hcp. But the ccp regions can be disrupted as is evident in Figure 7c. The mixing of various sizes and shapes leads to a disrupted ccp assembly with some nanoparticles fitting in where they can. This disordering is seen by the relatively straight cubic assembly beginning to curve as in Figure 4a. If this disruption continues, the resultant packing can begin to resemble hcp or even random packing.

Conclusion

We have recently been able to overcome the problem of large size and/or shape distributions found in aqueous colloidal solutions of platinum nanoparticles by several modifications in the preparation of the two-dimensional monolayers. Colloidal solutions with various shape and size distributions have been synthesized using acrylic acid as the capping material to allow for closest packing. But, the most notable of these enhancements is the addition of dodecanethiol to the colloidal solution which allows these nanoparticles to form self-assembled monolayers (SAMs) irrespective of the size or shape distributions. Solutions with one dominant shape (cubic), but a wide size distribution display a different type of organization than solutions with a narrow size distribution but many various shapes. Cubic closest packing (ccp) is achieved for cubic nanoparticles with a narrow size distribution. This packing is disrupted in regions with a large size distribution or with a mixture of shapes. Hexagonally closest packed assembly (hcp) is evident in areas where the shape of the nanoparticles differs or in size-segregated regions of very small nanoparticles (relative to the thiol). It seems that thiol, besides being involved in stabilizing the interparticle coupling, could slow down the rate of water evaporation to allow particles of different shapes or sizes to assemble in the most energetically favorable manner.

Acknowledgment. The authors thank the support of the National Science Foundation (CHE-9727633) and the Georgia Tech Microscopy Center for providing the research facilities

used in the characterization of these samples. J.P. and T.G. gratefully acknowledge partial support of this project by the Georgia Institute of Technology Molecular Design Institute, under prime contract N00014-95-1-1116 from the Office of Naval Research.

References and Notes

(1) Giersig, M.; Mulvaney, P. *Langmuir* **1993**, *9*, 3408.
(2) Mirkin, C. A.; Letsinger, R. L.; Mucic, R. C.; Storhoff, J. J. *Nature* **1996**, *382*, 607
(3) Brust, M.; Bethell, D.; Schiffrin, D. J.; Kiely, C. J. *Adv. Mater.* **1995**, *7*, 795.
(4) Murray, C. B.; Kagan, C. R.; Bawendi, M. G. *Science* **1995**, *270*, 1335.
(5) Motte, L.; Billoudet, F.; Lacaze, E.; Douin, J.; Pileni, M. P. *J. Phys. Chem.* **1997**, *101*, 138
(6) Whetten, R. L.; Khoury, J. T.; Alvarez, M. M.; Murthy, S.; Vezmar, I.; Wang, Z. L.; Stephens, P. W.; Cleveland, C. L.; Luedtke, W. D.; Landman, U. *Adv. Mater.* **1996**, *8*, 428.
(7) Pileni, M. P. *Langmuir* **1997**, *13*, 3266.
(8) Ahmadi, T. S.; Wang, Z. L.; Green, T. C.; Henglein, A.; El-Sayed, M. A. *Science* **1996**, *272*, 1924
(9) Ahmadi, T. S.; Wang, Z. L.; Henglein, A.; El-Sayed, M. A. *Chem. Mater.* **1996**, *8*, 1161.
(10) Petroski, J. M.; Wang, Z. L.; Green, T. C.; El-Sayed, M. A. *J. Phys. Chem. B* **1998**, *102*, 3316.
(11) Ohara, P. C.; Leff, D. V.; Heath, J. R.; Gelbart, W. M. *Phys. Rev. Lett.* **1995**, *75*, 3466
(12) Kiely, C. J.; Fink, J.; Brust, M.; Bethell, D.; Schiffrin, D. J. *Nature* **1998**, *396*, 444.
(13) Meakin, P. *Phys. Rev. Lett.* **1983**, *51*, 1119.
(14) Schaefer, D. W.; Martin, J. E.; Wiltzius, P.; Cannell, D. S. *Phys. Rev. Lett.* **1984**, *52*, 2371
(15) Ball, R. C.; Weitz, D. A.; Witten, T. A.; Leyvraz, F. *Phys. Rev. Lett.* **1987**, *58*, 274.
(16) Kolb, M.; Botet, R.; Julien, R. *Phys. Rev. Lett.* **1983**, *51*, 1123.
(17) Rampino, L. D.; Nord, F. F. *J. Am. Chem. Soc.* **1942**, *63*, 2745.
(18) Henglein, A.; Ershov, B. G.; Malow, M. *J. Phys. Chem.* **1995**, *99*, 14129.
(19) Wang, Z. L.; Harfenist, S. A.; Whetten, R. L.; Bentley, J.; Evans, N. D. *J. Phys. Chem. B* **1998**, *102*, 3068.
(20) Korgel, B. A.; Fullam, S.; Connolly, S.; Fitzmaurice, D. *J. Phys. Chem. B* **1998**, *102*, 8379
(21) Whetten, R. L.; Shafigullin, M. N.; Khoury, J. T.; Schaaff, T. G.; Vezmar, I.; Alvarez, M. M.; Wilkinson, A. *Acc. Chem. Res.* **1999**, *32*, 397.